

JAERI-M

9 5 7 7

PHYSICAL DESIGN CONSIDERATIONS OF THE  
NEXT TOKAMAK FUSION REACTOR  
— PARAMETER SURVEY OF THE DEVICE SIZE —

July 1981

Noboru FUJISAWA and Masayoshi SUGIHARA

日 本 原 子 力 研 究 所  
Japan Atomic Energy Research Institute

この報告書は、日本原子力研究所が JAERI-M レポートとして、不定期に刊行している研究報告書です。入手、複製などのお問い合わせは、日本原子力研究所技術情報部（茨城県那珂郡東海村）あて、お申しこしてください。

JAERI-M reports, issued irregularly, describe the results of research works carried out in JAERI. Inquiries about the availability of reports and their reproduction should be addressed to Division of Technical Information, Japan Atomic Energy Research Institute, Tokai-mura, Naka-gun, Ibaraki-ken, Japan.

Physical Design Considerations of the Next Tokamak Fusion Reactor

— Parameter Survey of the Device Size —

Noboru FUJISAWA and Masayoshi SUGIHARA

Division of Large Tokamak Development,  
Tokai Research Establishment, JAERI

(Received June 26, 1981)

Wide range of parameter surveys on the next device to JT-60 are made. Various physical and engineering requirements are taken into account, e.g., self-ignition, available maximum beta value, total fusion power, neutron wall loading,  $\alpha$ -particle confinement, heat flux to divertor plate, structural restriction on aspect ratio, device size, maximum toroidal magnetic field and so on. Since the energy confinement scaling law has ambiguities, emphases are placed on the methodology to determine the plasma and device parameters realizing the various objectives of the next device.

Keywords; Tokamak Fusion Reactor, Parameter Survey, Self-ignition Condition,  
Neutron Wall Loading, Plasma Engineering

次期トカマク核融合炉の物理設計  
—装置サイズのパラメータサーベイ—

日本原子力研究所東海研究所大型トカマク開発部  
藤沢 登・杉原正芳

(1981年6月26日受理)

JT-60の次に建設が計画されている次期装置の装置サイズについて広範囲なパラメータ・サーベイを行なった。その際にいろいろな物理的および工学的要求が考慮に入れられた。例えば、自己点火条件、到達可能最大ベータ値、全核融合出力、中性子壁面負荷、 $\alpha$ 粒子閉じ込め性能、ダイバータ板への熱流束、アスペクト比に対する装置構造上の制約、装置サイズ、最大トロイダル磁場等である。エネルギー閉じ込めスケーリング則には不確かさがあるため、次期装置に設定されたいろいろな目標を実現する装置およびプラズマのパラメータを設定するための方法論に重点を置いた。

## Contents

1. Introduction .....	1
2. Major roles required for the next device and requisites for its core plasma .....	1
3. Rough estimation of fundamental plasma parameters meeting the technical objectives .....	3
4. Detailed discussions of plasma parameters and device size	
4.1 Basis for selecting the parameters .....	9
4.2 General discussions of parameter survey of plasma parameters and device size .....	10
4.3 Detailed parameter survey of plasma parameters and device size ..	13
4.4 Determination of plasma parameters and device size .....	19
Acknowledgement .....	28
References .....	28

## 目 次

1. 序 論.....	1
2. 次期装置の主要な役割とプラズマに対する要求.....	1
3. 技術目標を達成するための基本プラズマパラメータの概略検討.....	3
4. プラズマおよび装置パラメータの詳細検討.....	9
4.1 パラメータ選定の基準.....	9
4.2 プラズマおよび装置サイズのパラメータ・サーベイの一般論.....	10
4.3 プラズマおよび装置サイズの詳細なパラメータ・サーベイ.....	13
4.4 プラズマパラメータおよび装置サイズの決定.....	19
謝 辞.....	28
文 献.....	28

## 1. Introduction

Recent remarkable progress in tokamak research predicts that scientific feasibility of thermonuclear reacted plasmas could possibly be realized in the middle of 1980's. JT-60 is scheduled to be in operation in 1984, and is expected to reach its critical condition with hydrogen plasmas in 1985. In the world, TFTR and JET are also scheduled to demonstrate scientific feasibility of DT plasmas at the same time as or earlier than JT-60.

In these circumstances, conceptual design studies of the next device as a step succeeding JT-60 are making progress, and at the same time we work actively on INTOR workshops under the auspice of IAEA.

In this report, we review the role to be imposed on the next device, and develop a physical design methodology for the next device, and determine the major plasma parameters meeting the objectives through the parameter study as an example.

## 2. Major roles required for the next device and main requisites for its core plasma

Research and development in the nuclear fusion have been making progress step by step by constructing devices which include technologies developed by then, and a future plan is also scheduled to take the same way; i.e., an experimental reactor, a demonstration reactor, a proto-type reactor, a commercial reactor and so forth. The demonstration reactor which would be constructed at the beginning of the 21st would have to demonstrate the reliable operation of a tokamak-type reactor. The next device, which we refer as the experimental reactor, is an important step placed on the way from JT-60 to the demonstration reactor.

In the next device, well controlled reacting plasmas have to be demonstrated to be in operation with high reliability by plasma control techniques which will be developed experimentally and theoretically. Moreover, the technologies such as superconducting magnet and remote handling, which are now under development, have also to be demonstrated to work well reliably. Another important role of the next device is an over-all test of technologies required for the demonstration reactor.

INTOR is now being designed just as the next device. The programmatic objectives of INTOR have been adopted on a base of experimental results, which

## 1. Introduction

Recent remarkable progress in tokamak research predicts that scientific feasibility of thermonuclear reacted plasmas could possibly be realized in the middle of 1980's. JT-60 is scheduled to be in operation in 1984, and is expected to reach its critical condition with hydrogen plasmas in 1985. In the world, TFTR and JET are also scheduled to demonstrate scientific feasibility of DT plasmas at the same time as or earlier than JT-60.

In these circumstances, conceptual design studies of the next device as a step succeeding JT-60 are making progress, and at the same time we work actively on INTOR workshops under the auspice of IAEA.

In this report, we review the role to be imposed on the next device, and develop a physical design methodology for the next device, and determine the major plasma parameters meeting the objectives through the parameter study as an example.

## 2. Major roles required for the next device and main requisites for its core plasma

Research and development in the nuclear fusion have been making progress step by step by constructing devices which include technologies developed by then, and a future plan is also scheduled to take the same way; i.e., an experimental reactor, a demonstration reactor, a proto-type reactor, a commercial reactor and so forth. The demonstration reactor which would be constructed at the beginning of the 21st would have to demonstrate the reliable operation of a tokamak-type reactor. The next device, which we refer as the experimental reactor, is an important step placed on the way from JT-60 to the demonstration reactor.

In the next device, well controlled reacting plasmas have to be demonstrated to be in operation with high reliability by plasma control techniques which will be developed experimentally and theoretically. Moreover, the technologies such as superconducting magnet and remote handling, which are now under development, have also to be demonstrated to work well reliably. Another important role of the next device is an over-all test of technologies required for the demonstration reactor.

INTOR is now being designed just as the next device. The programmatic objectives of INTOR have been adopted on a base of experimental results, which

are expected to be obtained in JT-60, JET and TFTR. They have also been adopted on the basis of the requirements from the demonstration reactor side. They are described in the zero phase report of INTOR, and their essentials are as follows.<sup>1)</sup>

- a) INTOR should be the maximum reasonable step beyond the next generation of large tokamaks (TFTR, JET, JT-60, T-15) in the world fusion programme.
- b) INTOR should demonstrate the plasma physics requirements for DEMO.
- c) INTOR should demonstrate those technologies required for DEMO that must be incorporated as an intrinsic part of the reactor (e.g., superconducting magnets, remote handling technology).
- d) INTOR should be a test facility for blanket, tritium production, plasma engineering, materials and other technology developments required for DEMO.
- e) INTOR should serve as a test and demonstration facility for magnetic fusion technology in general.
- f) INTOR should demonstrate the reliable operation of a fusion reactor.

These programmatic objectives can be applied to the next device ensuing JT-60. The item (a), however, somewhat controversial. It is questionable whether the "maximum" reasonable step is the best one. It depends on a strategy of how to overcome difficulties with the tokamak research.

We have also to remember that JT-60 lacks the research on DT burning. Hence, it is important for the next device not only to demonstrate the unified plasma control technologies developed by then, but also to make a research toward a more improved plasma performance, which has properly to include innovative technologies like a current sustain by RF.

The research on plasma physics seems to be incompatible with the engineering tests for the demonstration reactor. The concept of a staged operation may resolve this problem, that is, the plasma physics research could be concentrated on in the early phase of an operation period of the next device, and the remainder period would be devoted to the engineering tests.

Taking the above programmatic objectives into consideration, we have selected the major technological objects of the next device as follows.

- (1) Self-ignited DT plasmas.
- (2) Long-time burn more than 100 s.
- (3) Around 1 MW/m<sup>2</sup> in the wall loading
- (4) More than 1.0 in breeding ratio
- (5) Over 20 % in availability



The long burn pulse more than 100 s requires various kinds of the plasma control technologies, such as a burn temperature control, an impurity control, an equilibrium control and a stability control. The latter three control technologies will be completed to a great extent through the experimental research in JT-60. Their efficacy could be demonstrated in the next device.

The self-ignition in DT and its burn control, which will not be studied in JT-60 directly, will have some uncertainty. We will have to obtain effective technologies for them as soon as possible after starting the operation of the next device.

The pulsive operation in the tokamak-type device not only lessens the reactor's availability, but also increase the device dimension due to a repetition stress which requires stronger structure than in a steady operation. The research and development for a discharge current sustain by RF in a tokamak is scheduled to be in the JT-60 program. The application of the current sustain to the next device depends on the degree of its progress in JT-60. The direct current operation is a very favorable technology for the next machine, but is not necessarily indispensable, because the long burn pulse more than 100 s is possible with an air-core transformer method, which, however, makes a reactor structure more complicated. For the future tokamak-type devices ensuing the next device, the dc operation is absolutely indispensable.

Judging from the programmatic objectives imposed on the next device, needless to say, the wall loading and the availability are required to some extent. Both around  $1 \text{ MW/m}^2$  in the wall loading and more than 20 % in the availability are reasonable from the view point of an engineering test facility. Regarding the tritium, Japan has difficulty in its procurement. In this context, the requirement of more than 1.0 in the breeding ratio is a crucial item imposed on the next device.

The selection of plasma parameters, which satisfy the above technological objectives, will be described in the following sections.

### 3. Rough estimation of fundamental plasma parameters meeting the technical objectives

It is important to know what kinds of restraints have influences on a determination of fundamental plasma parameters satisfying the technical objectives in the last chapter, and to understand what ranges of plasma parameters meet the above objectives. Here, we are going to develop a rough estimation

The long burn pulse more than 100 s requires various kinds of the plasma control technologies, such as a burn temperature control, an impurity control, an equilibrium control and a stability control. The latter three control technologies will be completed to a great extent through the experimental research in JT-60. Their efficacy could be demonstrated in the next device.

The self-ignition in DT and its burn control, which will not be studied in JT-60 directly, will have some uncertainty. We will have to obtain effective technologies for them as soon as possible after starting the operation of the next device.

The pulsive operation in the tokamak-type device not only lessens the reactor's availability, but also increase the device dimension due to a repetition stress which requires stronger structure than in a steady operation. The research and development for a discharge current sustain by RF in a tokamak is scheduled to be in the JT-60 program. The application of the current sustain to the next device depends on the degree of its progress in JT-60. The direct current operation is a very favorable technology for the next machine, but is not necessarily indispensable, because the long burn pulse more than 100 s is possible with an air-core transformer method, which, however, makes a reactor structure more complicated. For the future tokamak-type devices ensuing the next device, the dc operation is absolutely indispensable.

Judging from the programmatic objectives imposed on the next device, needless to say, the wall loading and the availability are required to some extent. Both around  $1 \text{ MW/m}^2$  in the wall loading and more than 20 % in the availability are reasonable from the view point of an engineering test facility. Regarding the tritium, Japan has difficulty in its procurement. In this context, the requirement of more than 1.0 in the breeding ratio is a crucial item imposed on the next device.

The selection of plasma parameters, which satisfy the above technological objectives, will be described in the following sections.

### 3. Rough estimation of fundamental plasma parameters meeting the technical objectives

It is important to know what kinds of restraints have influences on a determination of fundamental plasma parameters satisfying the technical objectives in the last chapter, and to understand what ranges of plasma parameters meet the above objectives. Here, we are going to develop a rough estimation

using the simplest model, which, however, does not lose the essence.

First, a core plasma has to be self-ignited. The core plasma is assumed to be heated only by  $\alpha$ -particles of 3.5 MeV produced by D-T reactions. The loss from the plasma is also assumed to be the sum of a bremsstrahlung ( $P_{br}$ ) and a transport loss ( $P_{tr}$ ), and the latter is expressed by a confinement time ( $\tau_E$ ). The self-ignition can, therefore, be presented as

$$P_{\alpha} = P_{br} + P_{tr} \quad ,$$

where

$$P_{\alpha} = f(\bar{T}) \bar{n}^2 \quad ,$$

$$P_{br} = g(\bar{T}) \bar{n}^2 \quad ,$$

$$P_{tr} = \frac{C \bar{n} \bar{T}}{\tau_E} \quad .$$

The density and temperature are the averaged values measured in  $\bar{n}$  ( $10^{20} \text{ m}^{-3}$ ) and  $\bar{T}$  (keV), respectively.  $C$  is a numerical constant of  $4.8 \times 10^4$ . We also assume the core plasma to be a circular cross-section.

The above self-ignition condition can be transformed into the well-known  $\bar{n} \tau_E - \bar{T}$  relation, that is,

$$\bar{n} \tau_E = \frac{C \bar{T}}{\alpha f(\bar{T}) - g(\bar{T})}$$

According to more detailed calculations, in which profiles of density and temperature are taken into account, it is found that the  $\alpha$ -heating becomes very strong near the center of the core plasma. This effect is taken in the  $\alpha$ -heating power as  $\alpha$ .  $\alpha$ , usually, is 1.5 - 2.5 and in this analysis  $\alpha = 2$  is assumed.

Parametric dependence of  $\tau_E$  on density, temperature, radius and so on is very important in evaluating the major plasma parameters. There is a possibility that the different scaling of  $\tau_E$  leads to the different major parameters. Up to now, there is no confirmed  $\tau_E$ -scaling, which is applicable to ignited plasmas. It seems to be the best that Alcator scaling law is adopted as the confinement time scaling, which can explain well most tokamak experiments.

$$\tau_E = \bar{n} a^2 \quad .$$

Hence, the relation satisfying the self-ignited condition becomes

$$a^2 \bar{n}^2 = \frac{C \bar{T}}{\alpha f(\bar{T}) - g(\bar{T})}$$

Secondly,  $\beta$  value is a physically crucial restraint which has to be imposed on the ignited plasmas.  $\beta$  (%) can be written as

$$\beta = 8 \frac{\bar{n} \bar{T}}{B^2},$$

where  $B$  (T) is the toroidal field strength. Inserting the above self-ignition relation, the following relation is obtained,

$$a B^2 \beta = 8 \bar{T} \left( \frac{C \bar{T}}{\alpha f(\bar{T}) - g(\bar{T})} \right)^{\frac{1}{2}}.$$

The relation between  $\bar{T}$  and  $aB^2\beta$  is plotted in Fig. 3.1. It is evident that the value of  $aB^2\beta$  has its minimum at the temperature of (8~11) keV.

According to theoretical investigations the maximum  $\beta$  value of elongated plasmas is predicted to be limited to several percent, when ballooning modes are the dominant limiting factor in high  $\beta$  plasmas.<sup>2)</sup> On the other hand, experimental results show that the maximum  $\beta$  of 2~3 % is obtained even in circular plasmas so far.<sup>3)</sup> Unfortunately, it is uncertain whether or not the  $\beta$  value of several % can be attained in elongated discharges as theoretical predictions. Hence, in this context, it is reasonable to take the maximum  $\beta$  value as small as possible from the physical view point.

From the engineering point of view, it is natural that both  $a$  and  $B$  are as small as possible. Since both the larger machine size and the stronger magnetic field strength result in higher cost and more enhanced difficulties in engineering aspect.

According to the above discussions, the minimization of the value of  $aB^2\beta$  is favorable for the next device from the physical and engineering points of view. Therefore, a choice of the working temperature of (8-11) keV mitigates the most crucial physical difficulty in realization of high  $\beta$  plasma, and lessens the engineering hardness in strong toroidal magnetic field and large plasma radius.

The third restriction imposed on the core plasma is the wall loading. This comes out from the role as a test facility, which is one of the main objectives for the next device. Here, we refer the wall loading as a neutron power flux per unit area on a plasma surface. Then, the wall loading  $P_W$  (MW/m<sup>2</sup>) is

$$P_W = 2\alpha a P_\alpha.$$

Using the self-ignited relation, we have

$$P_W = \frac{4}{a} \alpha f(\bar{T}) \frac{C \bar{T}}{\alpha f(\bar{T}) - g(\bar{T})}$$

The relation between  $aP_W$  and  $\bar{T}$  is shown in Fig. 3.2.  $aP_W$  has its minimum at a temperature of (6 ~ 7) keV.

Lastly, the total thermal output  $P_T$  (MW), which however, is not the restriction here, can be easily calculated.

$$\begin{aligned} P_T &= 2\pi^2 a^2 R \times 5\alpha P_\alpha \\ &= 20\pi^2 R \alpha f(\bar{T}) \frac{C \bar{T}}{\alpha f(\bar{T}) - g(\bar{T})} \end{aligned}$$

The relation between  $P_T/2\pi R$  and  $\bar{T}$  is just the same as the one in Fig. 3.2.

It is evident that the total thermal output per unit length of the torus depends only on the temperature, and that the minimum value is 7 (MW/m).

Taking account of engineering constraint on space between the symmetric axis and a plasma, such as poloidal coils, toroidal coils, shieldings, blankets and vacuum chamber, the minimum major radius approaches to  $R \approx 5$  m. Then the minimum total output becomes 220 MW. Note that the tokamak-type reactor, which satisfies the self-ignited condition, has to have its minimal total thermal output of a few hundred MW, so long as the confinement time has the above mentioned scaling law. Hence, the first wall has to receive about a half hundred MW in thermal power flux except for the neutron wall loading. How successfully such a large thermal power flux can be handled without serious damages to the first wall is one of crucial items to be solved.

The relations among the major parameters ( $\bar{T}$ ,  $\beta$ ,  $a$ ,  $B$ ,  $P_W$ ), which satisfy the technical objectives imposed on the next device, have been derived in the above. Hereafter, the reasonable values of the major parameters in the next device will be roughly estimated. It seems to be natural for the next device that the temperature of 10 keV is adopted, since at this temperature the value of  $aB^2\beta$  becomes minimal as shown in Fig. 3.2. Then, two relations are obtained.

$$aB^2\beta = 103$$

$$aP_W = 1.06$$

When  $a$  is eliminated,

$$B^2\beta = 97 P_W .$$

Fig. 3.3 shows the relation between  $\beta$  and  $B$  as a parameter of  $P_W$ . From the figure, we can obtain a typical set of parameters;

$$B = 5 \text{ (T)}, \quad \beta = 4 \text{ (\%)}, \quad P_W = 1 \text{ (MW/m}^2\text{)}$$

$$a = 1.1 \text{ (m)}, \quad \bar{n} = 1.1 \times 10^{20} \text{ m}^{-3}$$

It is fortunate that the selected major parameters are not unrealistic at least.

We have investigated what sorts of conditions have influences on the major parameters and what values are taken by them. The most influential relation is the confinement scaling, which has still, unfortunately, uncertainty in the parameter range of the ignited plasma. Note that the better confinement mitigates the difficulties in physics and engineering, and makes the next device more realistic.

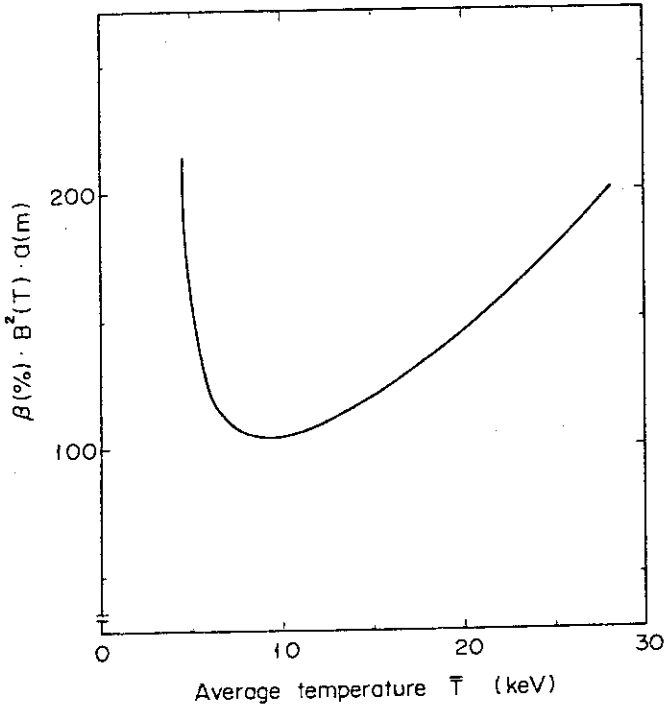


Fig. 3.1 The relation between average temperature  $\bar{T}$  and  $aB^2\beta$  to satisfy the self-ignition condition.

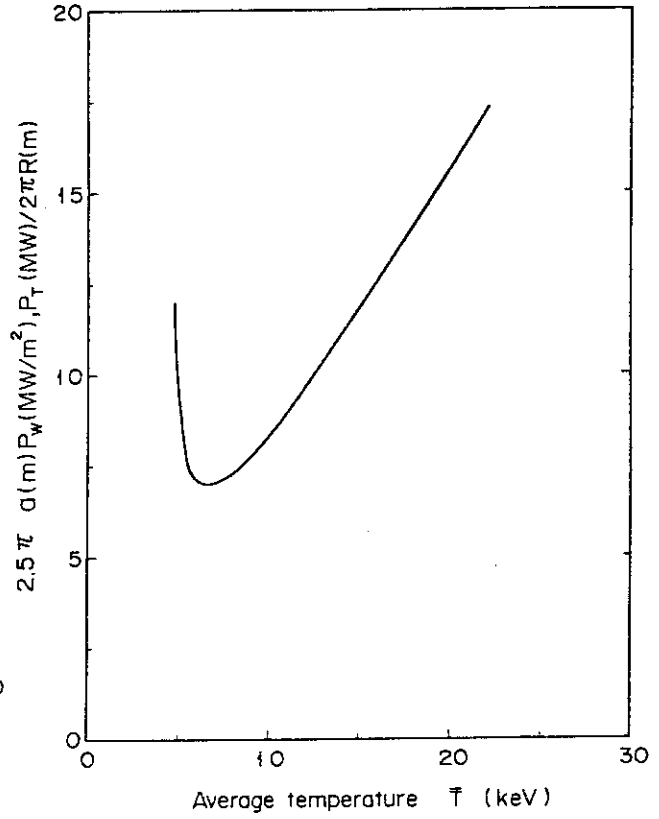


Fig. 3.2 The relation between average temperature  $\bar{T}$  and the neutron wall loading  $P_w$  multiplied by the plasma minor radius.

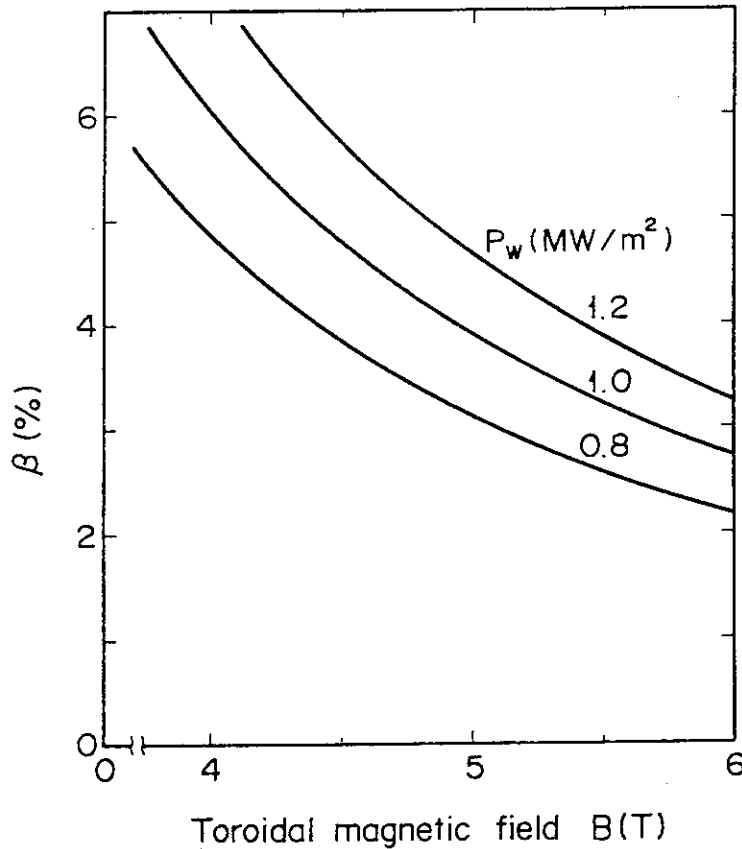


Fig. 3.3 The relations between beta value  $\beta$  and the toroidal magnetic field on axis  $B$  as a parameter of  $P_w$ .

## 4. Detailed discussions of plasma parameters and device size

## 4.1 Basis for selecting the parameters

We follow the basic ideas of Ref. 4 to determine the plasma and device parameters, which realize the various requirements both from physics and engineering. The outlines of the basic ideas are as follows. (1) We use the data of thermal conductivity and particle diffusion coefficient obtained mainly by the experiments in JFT-2 and JFT-2a. (2) Cool plasma layer surrounding the hot core plasma will inevitably be required to prevent the impurity contamination of the hot core plasma. The width of this layer will be 20~25 % of the plasma minor radius. (3) We use the poloidal divertor for the impurity control and ash exhaust. (4) Non-circular plasma with the elongation  $\kappa \sim 1.5$  should be employed to obtain a higher beta plasma.

More detailed discussions of the basis for selecting the plasma and device parameters of Ref. 4 are summarized in Table 4.1.

Table 4.1

Electron heat conductivity $\chi_e$	$4 \times 10^{19}/n_e$ ( $n_e$ : electron density)
Ion heat conductivity $\chi_i$	$2 \chi_{i \text{ neo}}$ ( $\chi_{i \text{ neo}}$ : neoclassical value)
Particle diffusion coefficient D	$\chi_e/2.5$
Width of cool plasma layer	$(0.2 \sim 0.25)a$
Noncircularity $\kappa$	1.5 (ellipticity)
Beta value	4 % (fuel) 5 % (total)
Heating	NBI 50 % (120 ~ 150 keV) RF 50 %
Divertor	Poloidal
Burn time	$\geq 100$ sec (DC operation if possible)
Toroidal field ripple	$\leq 0.75$ % (at plasma surface)



#### 4.2 General discussions of parameter survey of plasma parameters and device size

On the basis of the transport coefficients, beta limit considerations, etc. given in the previous section, we determine the plasma and device parameters. First, we derive the expressions for electron and ion energy confinement time. The hot core plasma is surrounded by the low temperature plasma layer with the thickness of  $(0.2 \sim 0.25)a$ , where  $a$  is the plasma minor radius. Assuming that the temperature profile in the hot core plasma is parabolic, the characteristic length of the temperature gradient  $L_T$  is given as

$$L_T = \frac{1}{T} \frac{\partial T}{\partial r} \sim 0.54a \quad . \quad (1)$$

We estimate the energy confinement time  $\tau_E$  by  $\tau_E \sim 1.5L_T^2/\chi$ . Then the energy confinement time for electrons and ions are given as

$$\tau_{Ee} \sim 1.1 \times 10^{-20} \bar{n}_e a^2 \quad , \quad (2)$$

$$\tau_{Ei} \sim 9.3 \times 10^{16} \frac{B^2 \sqrt{T}}{\bar{n}} a^2 \quad . \quad (3)$$

The basic equation for the determination of plasma and device parameters is the following simplified power balance equation.

$$\frac{3}{2} \bar{n} k \bar{T} \left( \frac{1}{\tau_{Ee}} + \frac{1}{\tau_{Ei}} \right) + P_{br} = \frac{1}{4} \bar{n}^2 \langle \sigma v \rangle E_\alpha f_r \left( 1 + \frac{5}{Q} \right) \quad , \quad (4)$$

where we have assumed that  $\bar{n}_D = \bar{n}_T = \bar{n}/2$  and  $\bar{T}_i = \bar{T}_e = \bar{T}$ . Only bremsstrahlung loss ( $P_{br} = 1.42 \times 10^{-38} \sqrt{\bar{T}} \bar{n}_e^2$ ) is considered for radiation loss. The numerical factor  $f_r$  represents the effect of the density and temperature profile on fusion power production and is assumed  $f_r \sim 1.5$  for parabolic like density and temperature profile. The external heating power is included in the form of  $Q$ , where  $Q = P_{in}/P_{fusion}$  is the energy multiplication factor.  $Q = \infty$  represents the self-ignition condition. Other notations are conventional ones.

First, we set the target temperature. This can be done from various view points. Beta value is one of the most important factor in physics and the maximum attainable beta value is uncertain at present. Thus, from physics view points, it should be desirable that the target temperature is chosen so that the required plasma performance can be realized by the minimal  $\beta$  value. From the engineering view points, we can choose the target temperature so that the

required plasma performance can be achieved by the minimal device size (minor radius). We can also choose the target temperature so that the required fusion power or neutron wall loading can be achieved with the minimal beta value or device size. Equation (4) contains three independent variables, if the magnetic field and the major radius are given. They are  $\bar{T}$  or  $a$  or  $\beta$  or  $P_T$  (total fusion power) or  $P_W$  (neutron wall loading). Thus, when we fix one of them, we obtain the relation between the remaining parameter and the temperature. For instance, the relation between  $\beta$  and  $\bar{T}$  with minor radius being fixed is given as

$$\beta^2 = \frac{1}{B^4} \frac{1.42 \times 10^{-34} \bar{T}^3}{a^2 [2.11 (1 + \frac{5}{Q}) \langle \sigma U \rangle - 1.42 \times 10^{-25} \sqrt{\bar{T}}] - \frac{2.58 \times 10^{-23} \sqrt{\bar{T}}}{B^2}} \quad (5)$$

Temperature dependences of  $a$ ,  $\beta$ ,  $P_T$  and  $P_W$  with other parameter being fixed are investigated and are summarized as follows.

- (1)  $a = \text{const. (1.1 m)}$       Fig. 4.1 ,
- (2)  $\beta = \text{const. (3 \%)}$       Fig. 4.2 ,
- (3)  $P_T = \text{const. (300 MW)}$       Fig. 4.3 ,
- (4)  $P_W = \text{const. (0.8 MW/m}^2\text{)}$       Fig. 4.4 .

In all of these figures,  $Q = \infty$ ,  $B = 5.5 \text{ T}$  and  $R = 5 \text{ m}$  are assumed. As can be seen from Figs. 4.1 and 4.2, the self-ignition condition can be achieved with minimal  $\beta$  value and minor radius when  $\bar{T} = 10 \sim 12 \text{ keV}$ . Total fusion power and neutron wall loading take their minimal values at about this temperature. When we fix the total fusion power or neutron wall loading to the target value, the minimal  $\beta$  value and minor radius are not achieved for the same temperature. For instance, Fig. 4.3 shows that  $\beta$  value and minor radius to achieve the self-ignition as well as 300 MW total fusion power take their respective maximum and minimal values at  $\bar{T} \sim 10 \text{ keV}$ .

After all the optimum temperature should be determined by the requirement or restriction condition, which we consider most important and critical. The most critical requirement and restriction from physics view points will be that the self-ignition should be achieved by the minimal  $\beta$  value. This is rather simple, while that from engineering view points will not be so simple. From the view points of mitigating the engineering difficulties of the device, the most important ones will be to make the device size small or to lower the heat load on the first wall / divertor plate. Another choice can be that a certain level of total fusion power or neutron wall loading should be maintained

for engineering tests. In the present, let us consider that making the device size small is more important. Fortunately, the optimum temperature by this requirement is almost the same as that by physics requirement, so that we set the target temperature to 10 keV.

We now proceed to the determination of the device parameters. This can be done by using Eq. (4) with the attainable  $\beta$  value and the required plasma performance (Q value) as parameters. The results are shown in Fig. 4.5, in which the relations between minor radius as well as total fusion power and the  $\beta$  value are given for  $B = 5.5$  T. Beta value varies with the toroidal magnetic field on axis, so that simple conversions of beta values for various B are shown in abscissa. Strictly speaking, this conversion is not correct, since Eq. (5) does not depend only on  $\beta^2 B^4$ , but contains  $B^2$  in energy loss term by ions. Although the latter term is relatively small, the conversion should be read as a reference. Total fusion power is calculated for  $R = 5$  m. Note that it is not realistic to fix  $R = \text{const}$  in spite of the variation of minor radius. We will make more realistic treatment of this in the later section. As is shown in this figure, the difference of the device size (minor radius) between  $Q = \infty$  and  $Q = 5 \sim 10$  is about 20 % at most. The total fusion power of the device of  $Q = \infty$ , however, is 1.5 to 2 times larger than that of  $Q = 5 \sim 10$ . While, the difference of the total heat load on the first wall / divertor plate between  $Q = \infty$  and  $Q = 5 \sim 10$  will be much smaller, since, in the low Q operation, large external heating power must be applied to the plasma. The solid line of Fig. 4.6 shows this situation. There is no appreciable difference between  $Q = \infty$  and  $Q = 5$ . This result is obtained by fixing  $R (= 5 \text{ m})$ . If we change  $R$  in accordance with a by detailed design studies, this difference may become slightly larger. For instance, if we change  $R$  in proportion to  $a$  (i.e. aspect ratio is constant;  $A = 4.5$ ), the difference becomes about 30 % as shown by broken lines in Fig. 4.6. Even in this case, however, the difference of the heat load on divertor plate may become very small. If we estimate the area of the divertor plate receiving the heat by  $R\lambda_s$  ( $\lambda_s$  : scrape-off layer width), the heat load on the divertor plate  $\Gamma_n$  ( $\propto P_T/R\lambda_s \propto P_T/R^{1.5}$ ) of  $Q = 5$  is larger than that of  $Q = \infty$  as shown by dotted lines in Fig. 4.6. This result is not necessarily decisive, since we must carefully examine the dependence of the tilting angle of the divertor plate and the conversion efficiency to radiation energy loss on the device size. In addition, it is not realistic to fix aspect ratio. At any rate, there should be no remarkable difference of the heat load between  $Q = \infty$  and  $Q = 5$ .

For the reasons mentioned above, it does not seem plausible that the engineering difficulties can be drastically mitigated in the device of  $Q = 5$  compared with that of  $Q = \infty$  from the view points of the device size and heat load. On the contrary, considering that large steady additional heating power is necessary in low  $Q$  operation, it is not preferable to aim at the device of such low  $Q$ . It should be appropriate to aim at the device of  $Q = \infty$ , since this will be the final target of tokamak reactor. Even in this case, however, we should provide some steady additional heating equipment to avoid the degradations of plasma performance due to any possible deterioration of the confinement. In addition, we would have to employ high  $Q$  ( $Q = 20 \sim 30$ ) driven operation, if proper burn control scheme could not be established.

#### 4.3 Detailed parameter survey of plasma parameters and device size

In Sec. 4.2, we have discussed the plasma and device parameters by setting the  $\beta$  value, toroidal magnetic field on axis and major radius to arbitrary values. Actually, however, available maximum  $\beta$  value does depend on the device parameters. The toroidal magnetic field on axis also depends on the aspect ratio and minor radius. Furthermore, there should exist a structural restriction on aspect ratio or major radius, which depends on the minor radius and aspect ratio itself through the required volt seconds. We must take account of these facts properly to determine the plasma and device parameters, which can realize the required plasma performance or total fusion power or neutron wall loading.

The device size can be expressed by minor radius and aspect ratio  $A$ . Thus when we rewrite various restricting conditions to  $a-A$  relations, we obtain the regions of the possible device size, which meet various physical and engineering requirements. This  $a-A$  diagram enables us systematic and wide range of parameter survey of the device. We will consider the following requirements and restriction conditions, which will be most essential. They are (1) Plasma performance ( $Q = 5 \sim \infty$ ), (2)  $\alpha$ -particle confinement, (3) restriction on aspect ratio, (4) total fusion power and neutron wall loading.

##### (1) Plasma performance

The plasma minor radius, which can realize the required plasma performances ( $Q$  value), is given from Eq. (1) as

$$a^2 = \frac{\frac{2.58 \times 10^{-23} \sqrt{\bar{T}}}{B^2} + \frac{1.42 \times 10^{-34} \bar{T}^3}{\beta^2 B^4}}{2.11 \left(1 + \frac{5}{Q}\right) \langle \sigma v \rangle - 1.42 \times 10^{-25} \sqrt{\bar{T}}} \quad (6)$$

The toroidal magnetic field on axis is expressed as

$$B = B_{\max} \left(1 - \frac{1 + \Delta/a}{A}\right) \quad , \quad (7)$$

where  $B_{\max}$  and  $\Delta$  are the maximum field at the inner surface of the toroidal field coil and the distance between the inner surfaces of toroidal coil and plasma (Fig. 4.7), respectively. Although smaller value of  $\Delta$  is preferable to obtain higher magnetic field on axis for the same value of  $B_{\max}$ , the minimum required value of  $\Delta$  is almost uniquely determined by the necessary space for scrape-off layer width, vacuum vessel, shielding, automatic assembly and so on. Furthermore, this value does not depend on  $a$  and  $A$  so strongly. We set  $\Delta$  to 1.2 ~ 1.5 m on the basis of the design studies of INTOR<sup>1)5)</sup> and other devices<sup>6)7)</sup>, and neglect its dependence on the device size.

The available maximum beta value  $\beta_{\max}$ , which is stable to ballooning instability, has been extensively studied numerically<sup>2)8)9)</sup>, and the scaling law for  $\beta_{\max}$  has been established as<sup>8)9)</sup>

$$\beta_{\max} = C_{\beta} q^{-0.54} (A-1)^{-0.76} \quad , \quad (8)$$

where  $q$  is the safety factor at the plasma surface.  $C_{\beta}$  is a numerical value and is given  $7.88 \times 10^{-2}$  for circular plasma. We will employ noncircular plasma to obtain higher  $\beta$  plasma. We set the noncircularity  $\kappa$  to 1.5, which will be around the compromised value between higher  $\beta$  value and the device size as well as the vertical stability. In this case, the numerical value  $C_{\beta}$  is about  $1.5 \times 10^{-1}$  by a simple extrapolation of the results given in Ref. (8). Smaller value of  $q$  is preferable to achieve higher  $\beta$  value, though the dependence of  $\beta_{\max}$  on  $q$  is rather weak. It is uncertain whether or not low  $q$  operation (i.e.  $q < 2$ ) without disruption is possible in near term tokamaks, so that we set  $q$  to 2.5 to avoid potential danger of frequent plasma disruption.

Substituting Eqs. (7) and (8) into Eq. (6), we obtain  $a$ - $A$  diagram determined by the requirement of plasma performance. The cases of  $Q = 5$  and  $\infty$  are shown by solid lines for  $B_{\max} = 11$  T in Fig. 4.8 and for  $B_{\max} = 10$  T in Fig. 4.9. In these calculations, we use  $\Delta = 1.5$  m,  $q = 2.5$  and  $\bar{T} = 10$  keV. Note that the plasma minor radius to achieve the required plasma performance

increases slightly as A becomes small, in spite of the fact that higher  $\beta$  value is achievable for smaller A. This is because the toroidal magnetic field on axis becomes smaller for small A.

### (2) $\alpha$ -particle confinement

It is necessary for  $\alpha$ -particles to be well confined in the device determined above. In particular, the confinement of  $\alpha$ -particles could become marginal in the device of low Q operation with small device size. Here, we will make a rough estimation for the orbit loss of  $\alpha$ -particles.

According to the numerical calculation of the orbit loss of  $\alpha$ -particles in non-circular plasma<sup>10)</sup>, the loss rate depends on the aspect ratio and the plasma current most strongly, so that we choose them as dominant parameters for the loss rate. We will estimate the loss rate at  $r = 0.75a$ , since about 90 % of  $\alpha$ -particles are produced within this point. We will consider this loss rate as a measure of the total loss of  $\alpha$ -particles. Following the results of Ref. (10), we obtain the expression of loss rate  $G_{\text{loss}}$  by fitting.

$$G_{\text{loss}} = 2.3 \times 10^{12} A^{-2.3} I_p^{-1.8} \quad , \quad (9)$$

where the plasma current is expressed as

$$I_p = \frac{2\pi}{\mu_0} \frac{aB}{qA} \frac{1+\kappa^2}{2} \quad . \quad (10)$$

Actually, however, this expression of  $I_p$  will considerably differ from that of actual toroidal configuration. Larger plasma current than that of Eq. (8) will be necessary to obtain the required q value. This effect will lead to more sufficient  $\alpha$ -particle confinement due to the strong dependence of  $G_{\text{loss}}$  on  $I_p$ .

The cases of  $G_{\text{loss}} = 0.5$  and  $0.2$  are shown by dotted lines in Figs. 4.8 and 4.9 for  $B_{\text{max}} = 11$  T and 10 T, respectively. We also use  $\kappa = 1.5$ , and  $\Delta = 1.5$  m. These loss rates will roughly correspond to 5 % and 2 % loss of total  $\alpha$ -particles, respectively. The orbit loss of  $\alpha$ -particles is negligibly small in the device of  $Q = \infty$ . Even in the device of  $Q = 5$ , the loss rate amounts to about 2 % at most.

### (3) Structural restriction of aspect ratio

The major radius R is represented as

$$R = r_v + r_c + a \quad , \quad (11)$$

where  $r_v$  is the required space for volt seconds (Fig. 4.7).  $r_c$  is the distance between the plasma inner surface and the inner surface of the poloidal field coils around the center column. This space is required for poloidal and toroidal coils, shielding, support structure and so forth. Although smaller  $r_c$  is desirable to make the device size compact, the minimum required value of  $r_c$  is, on the whole, uniquely determined by structural restriction. We set this value to  $2.6 \sim 3.0$  m on the basis of INTOR<sup>1)5)</sup> and other devices<sup>6)7)</sup>. Actually, this value will vary slightly with the changes of the toroidal magnetic field, bore size of the toroidal coils and so on, while we neglect this dependence for simplicity.

The value of  $r_v$  is determined by the required volt seconds for the full operation and the maximum poloidal magnetic field  $B_{pmax}$ . The required volt seconds consists of the inductive part  $\phi_i$  and the resistive part  $\phi_r$ . They are given as

$$\begin{aligned} \phi_i &= L I_p = \mu_0 R \left( \ln \frac{8R}{a} + \frac{\ell_i}{2} - 2 \right) \times \frac{2\pi}{\mu_0} \frac{a^2 B}{qR} \frac{1+\kappa^2}{2} \\ &\sim \frac{4\pi a^2 B}{q} \frac{1+\kappa^2}{2} \quad , \end{aligned} \quad (12)$$

$$\phi_r = \frac{4\pi}{\mu_0} \frac{1}{\kappa} \frac{1+\kappa^2}{2} \frac{B}{q_a} \int_0^{t_f} \frac{\eta(t)}{\tilde{q}(t)} dt \quad , \quad (13)$$

where  $q = q_a \tilde{q}(t)$  and  $\ell_i$  is internal inductance of the plasma.  $\eta$  and  $t_f$  are the resistivity of the plasma and the operation time (from breakdown to shutdown), respectively. Note that the time integral of Eq. (13) is determined by  $q$  value, operation temperature and operation scenario (i.e. scenario of the start up, burn and shutdown), and does not depend on the device size. Thus  $\phi_r$  depends on the device size only through  $B$ . Although further optimization of start up and burn scenario will be necessary, the scenario adopted in INTOR<sup>1)5)</sup> may be the typical one, so that we will also employ the same scenario as INTOR, for simplicity. In this case,  $\int_0^{t_f} \eta/\tilde{q} dt \sim 1.36 \times 10^{-6}$  by simple numerical evaluation, so that we obtain

$$\phi_r \sim 5.9 B_{max} \left( 1 - \frac{1+\Delta/a}{A} \right) \quad . \quad (14)$$

Actually, however, equilibrium magnetic field coils give a certain fraction of the required volt seconds to sustain the plasma current. Thus, the

total volt seconds applied to the inner most poloidal coils (OH coils) around the center column becomes smaller than that given by Eqs. (12) and (14). We simply estimate this effect by considering the vertical field only. The vertical field  $B_V$  required for plasma equilibrium is given as

$$B_V = \frac{\mu_0 I_p}{4\pi R} \left( \ln \frac{8R}{a} - \frac{1}{2} + \beta_p + \frac{l_i}{2} - 1 \right) \sim \frac{\mu_0 I_p}{4\pi R} (2.5 + \beta_p) \quad , \quad (15)$$

where  $\beta_p$  is the poloidal beta value. This value is related to  $\beta$  value and is expressed by using Eq. (8) as

$$\beta_p = q^2 A^2 \frac{2}{1+\kappa^2} \beta = 0.35 A^2 (A-1)^{-0.76} \quad . \quad (16)$$

Thus using Eqs. (10) and (16), Eq. (15) reduces to

$$B_V = 0.325 B_{\max} \left( 1 - \frac{1+\Delta/a}{A} \right) \frac{1}{A^2} [2.5 + 0.35 A^2 (A-1)^{-0.76}] \quad . \quad (17)$$

We assume that  $B_V$  is uniform for simplicity, so that  $r_V$  can be obtained by the following equation,

$$\pi r_V^2 B_{p\max} = \frac{1}{2} [ \phi_i + \phi_r - \pi B_V (R^2 - r_V^2) ] \quad . \quad (18)$$

Substituting Eq. (18) into Eq. (11), we obtain the equation for the structural restriction of aspect ratio as

$$A \geq \frac{1}{[\pi(B_{p\max} - B_V)]^{1/2}} \left[ \frac{1}{2} B_{\max} \left( 1 - \frac{1+\Delta/a}{A} \right) \left( 8.17 + \frac{5.88}{a^2} \right) - \frac{\pi}{2} A^2 B_V \right]^{1/2} + \frac{r_c}{a} + 1 \quad . \quad (19)$$

The cases of  $r_c = 2.6$  m and 3 m are shown by broken lines in Fig. 4.8 for ( $B_{\max} = 11$  T,  $B_{p\max} = 8$  T) and in Fig. 4.9 for ( $B_{\max} = 10$  T,  $B_{p\max} = 7$  T), respectively. Since Eq. (19) depends on  $B_{\max}$  and  $B_{p\max}$  as the form of square root of  $B_{p\max}/B_{\max}$ , this relation in Fig. 4.8 is almost the same as that in Fig. 4.9. We also find that the dependence of Eq. (19) on  $\Delta$  is very weak.

As mentioned before, the plasma current is considerably larger than that given by Eq. (10) for the  $q$  value correctly obtained by equilibrium calculations. This effect may alter the results considerably. More correct evaluation of  $r_V$  by taking account of this effect is now in progress. Another



important factor for the evaluation of  $r_v$  is RF current sustain. If this method were employed, the result would be greatly altered.

#### (4) Total fusion power and neutron wall loading

Total fusion power  $P_T$  and neutron wall loading  $P_W$  are expressed by using Eqs. (7) and (8) as

$$P_T = 4.36 \times 10^9 (A-1)^{-1.52} B_{\max}^4 \left(1 - \frac{1+\Delta/a}{A}\right)^4 a^3 A \quad , \quad (20)$$

$$P_W = 6.93 \times 10^7 (A-1)^{-1.52} B_{\max}^4 \left(1 - \frac{1+\Delta/a}{A}\right)^4 a \quad . \quad (21)$$

The  $a$ - $A$  relations to achieve the required  $P_T$  (400 and 200 MW) and  $P_W$  (1.0 and 0.6 MW/m<sup>2</sup>) are shown in Figs. 4.10 and 4.11 for  $B_{\max} = 11$  T and 10 T, respectively. The condition for self-ignition ( $Q = \infty$ ) and the restriction of aspect ratio ( $r_c = 3$  m) are shown in the same figures.

Figs. 4.10 and 4.11 provide the parameter regions of the device size, which can satisfy the self-ignition condition, achieve the required total fusion power and neutron wall loading and meet the requirement of the structural restriction on aspect ratio simultaneously.

To determine the target point in this region, we must give priority to some of the conditions or requirements and/or impose other requirements. We must follow the structural restriction on aspect ratio by all means. If emphases are placed on the self-ignition and the compactness of the device, we must find an optimum point, at which the most compact device is realized, on the curves of structural restriction and self-ignition. We take the plasma volume  $V$  and the radius of the plasma outer surface  $\tilde{R}$  as measures of the reactor size. The variations of  $V$  and  $\tilde{R}$  on these curves are shown in Fig. 4.12.  $\tilde{R}$  takes its minimum at  $A \sim 4.5$ , while  $V$  is nearly constant for  $A \geq 4.5$ . On the other hand, the bore size of the toroidal coils will increase with the plasma minor radius, so that the device with smaller aspect ratio is disadvantageous in this regard. After all, the device with  $A = 4.5 \sim 5$  and  $a = 1.1 \sim 1.2$  m will be the optimum one. Total fusion power and neutron wall loading are uniquely determined for such device ; i.e.  $P_T = 250 \sim 300$  MW and  $P_W = 0.7 \sim 0.8$  MW/m<sup>2</sup>.

As a matter of course, there should be various requirements besides the compactness ; e.g. the heat load on the first wall / divertor plate, the maximum toroidal field, electrical power of poloidal coil system and so forth. It will be possible to lower the heat load or maximum toroidal field if the

device size is enlarged. This can be investigated by selecting proper paths in the allowable region of Figs. 4.10 and 4.11. For example, the variation of the heat load on the divertor plate  $\Gamma_T$  ( $\propto P_T/(aA)^{1.5}$ ) evaluated on the same path as in Fig. 4.12 is shown in Fig. 4.13.  $\Gamma_T$  takes its maximum at  $A \sim 4.5$ , so that certain compromise will be required with the device size.

#### 4.4 Determination of plasma parameters and device size

On the basis of the general discussions mentioned so far, we will determine the device parameters concretely. We will give the fundamental priority to the realization of the self ignition condition and the compactness of the device size. In order to mitigate the engineering difficulties, we set the maximum toroidal field to about 10 T, so that we can use Fig. 4.11 as the base for selecting the device parameters. As mentioned before, the optimum device parameter, which realize the self-ignition condition and make the device size most compact, is obtained when  $A = 4.5 \sim 5.0$  and  $a = 1.1 \sim 1.2$  m. We select appropriate and consistent set of parameters from these regions. Typical example is shown in Table 4.2. In this set of parameters, we have chosen the beta value slightly higher than that determined by Eq. (8). This will be possible when we consider the finite Larmor radius effect and so on<sup>11)</sup>. As a result,  $P_T$  and  $P_W$  become larger than that obtained by using Eq. (8). This gives also some margin to the realization of the self ignition condition.

Table 4.2

Major radius	R		5.3 m
Minor radius	a/b		1.1 / 1.65 m
Noncircularity	$\kappa$		1.5
Toroidal field on axis	B		5.2 T
Plasma current	$I_p$		3.9 MA
Safety factor	$q_a$		2.5
Q value			$\geq 30$
Total fusion power	$P_T$		420 MW
Neutron wall loading	$P_W$		1 MW/m <sup>2</sup>
Burn time			$\geq 100$ sec
Average temperature			10 keV
" density			$1.1 \times 10^{20}$ m <sup>-3</sup>
Toroidal beta value			4 %
Additional heating		NBI	25 ~ 30 MW
		RF	25 ~ 30 MW
Impurity control, ash exhaust		Poloidal divertor	

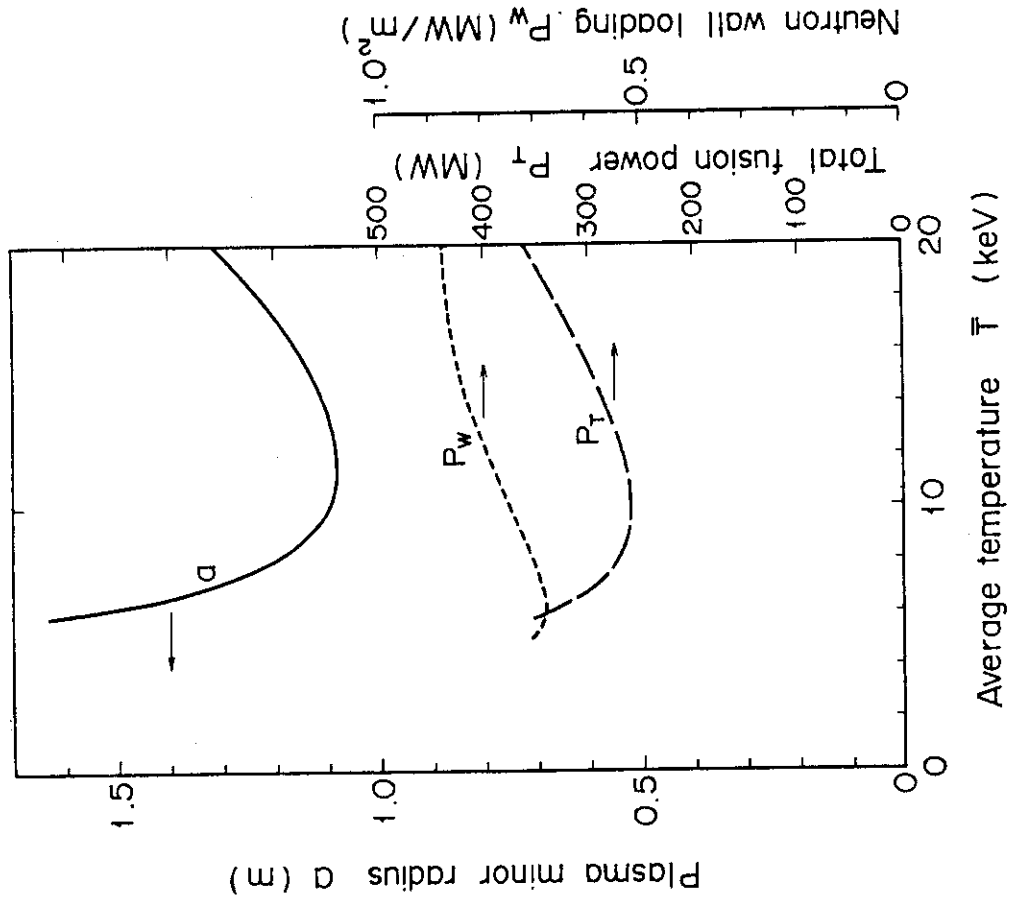


Fig. 4.1 Temperature dependences of  $\beta$ ,  $P_T$  and  $P_W$  with a being fixed ( $a=1.1m$ ).  $Q=\infty$ ,  $B=5.5T$  and  $R=5m$  are assumed.

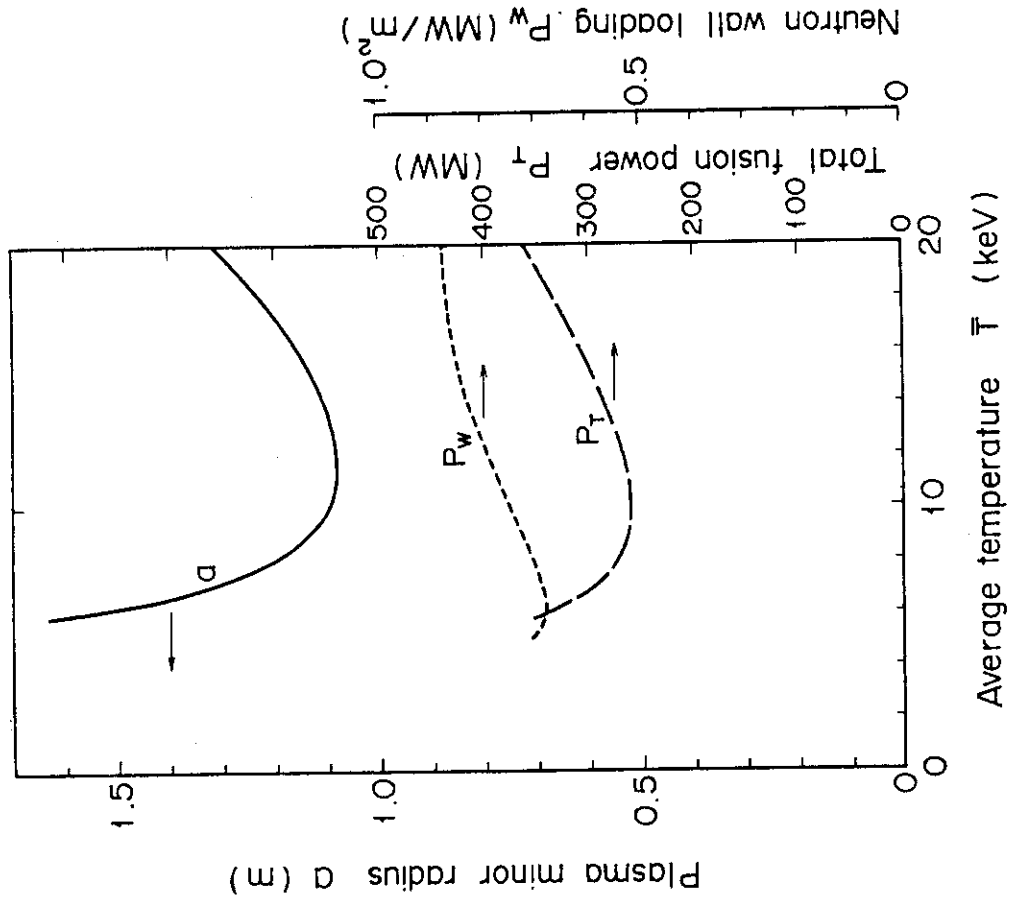


Fig. 4.2 Temperature dependences of  $a$ ,  $P_T$  and  $P_W$  with  $\beta$  value being fixed ( $\beta=3\%$ ).  $Q=\infty$ ,  $B=5.5T$  and  $R=5m$  are assumed.

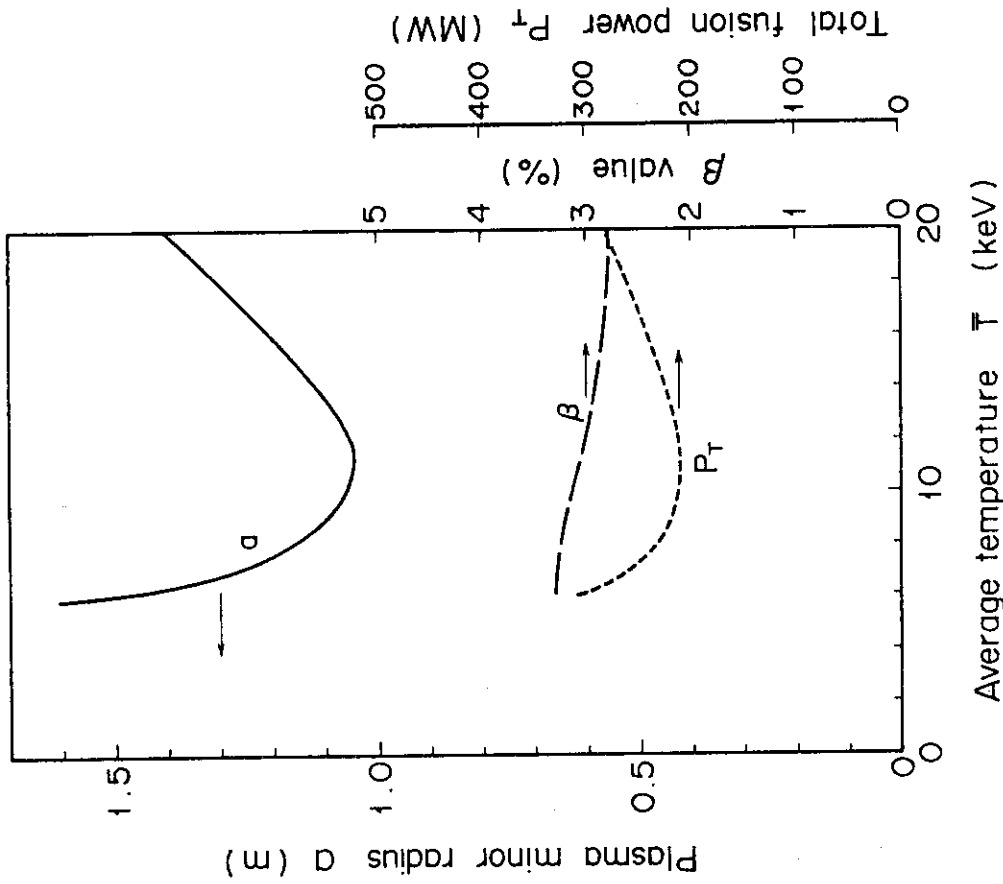


Fig. 4.3 Temperature dependences of  $a$ ,  $\beta$  and  $P_w$  with  $P_T$  being fixed ( $P_T=300\text{MW}$ ).  $Q=\infty$ ,  $B=5.5\text{T}$  and  $R=5\text{m}$  are assumed.

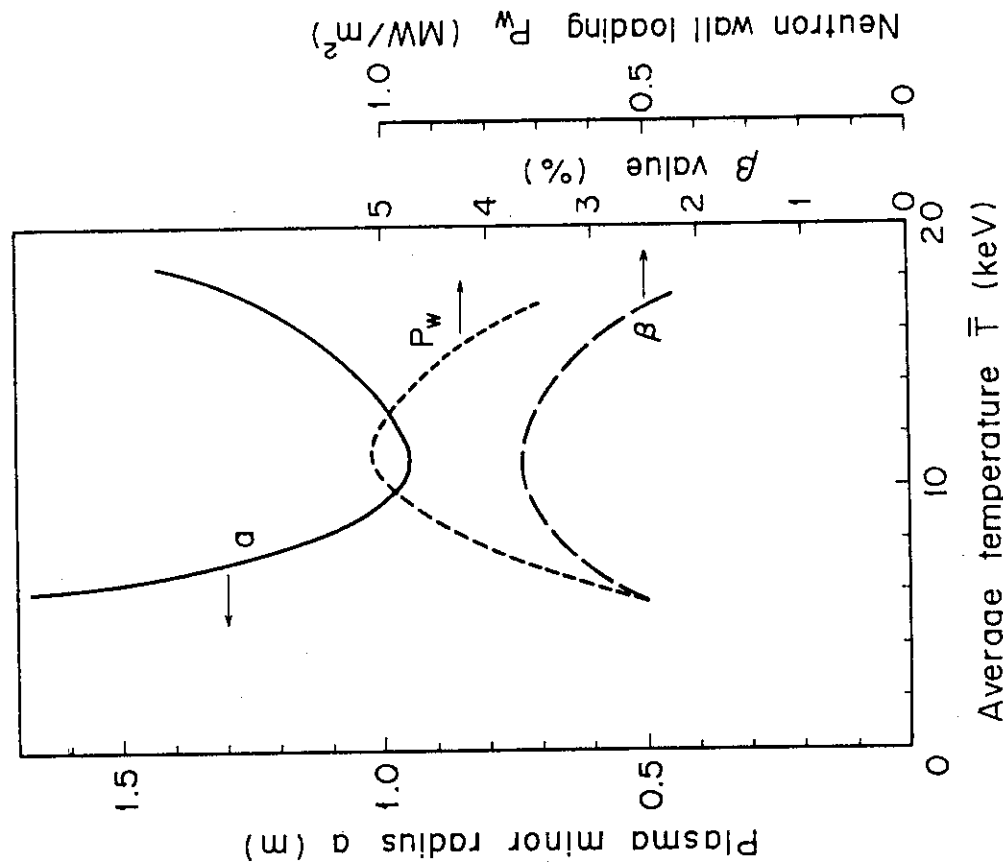


Fig. 4.4 Temperature dependences of  $a$ ,  $\beta$  and  $P_T$  with  $P_w$  being fixed ( $P_w=0.8\text{MW/m}^2$ ).  $Q=\infty$ ,  $B=5.5\text{T}$  and  $R=5\text{m}$  are assumed.

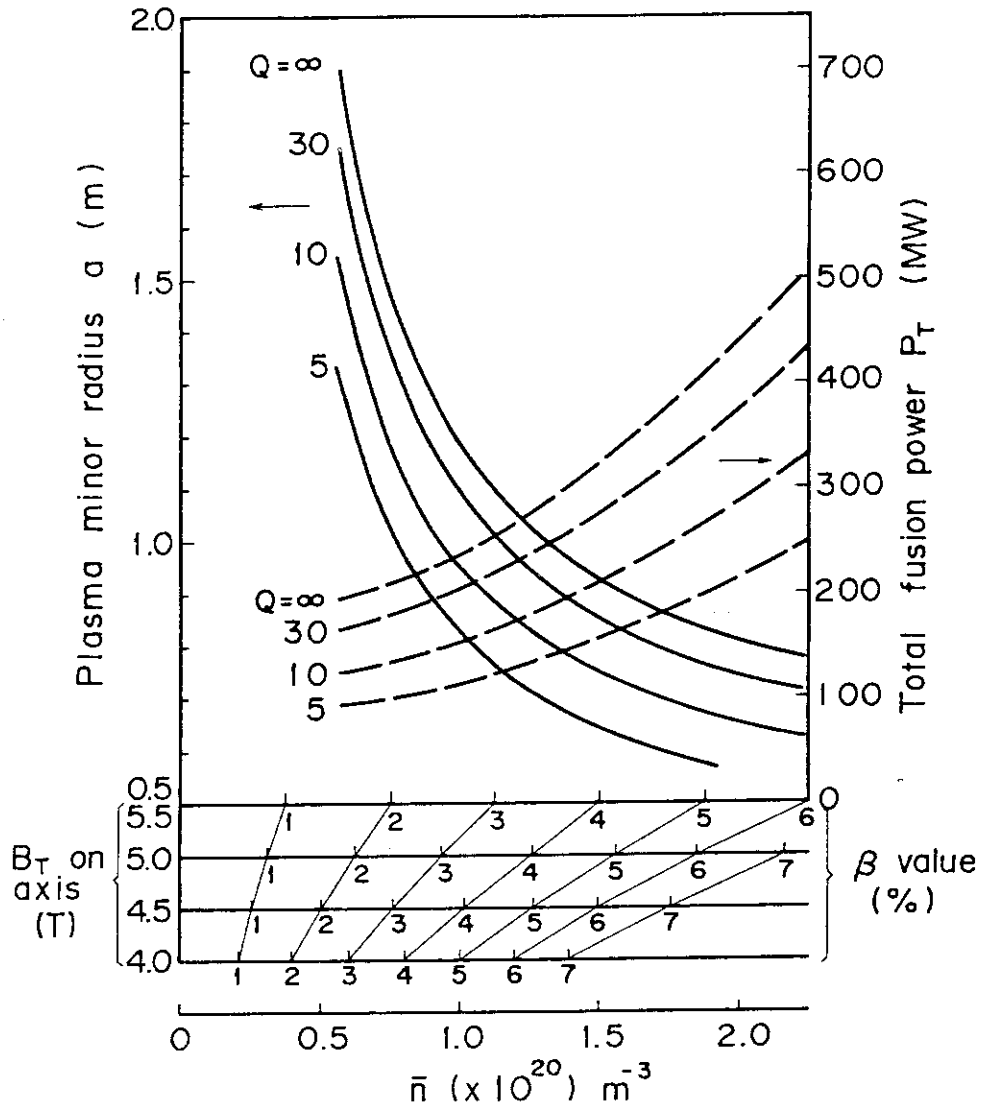


Fig. 4.5 Plasma minor radius to realize the required plasma performance (Q value) as a function of  $\beta$  value. Toroidal magnetic field is assumed  $B=5.5\text{T}$ . Simple conversions of the  $\beta$  value for various B are shown in abscissa. Total fusion power  $P_T$  is also shown for various Q values. In this calculation,  $R=5\text{m}$  and  $\kappa=1.5$  are assumed.

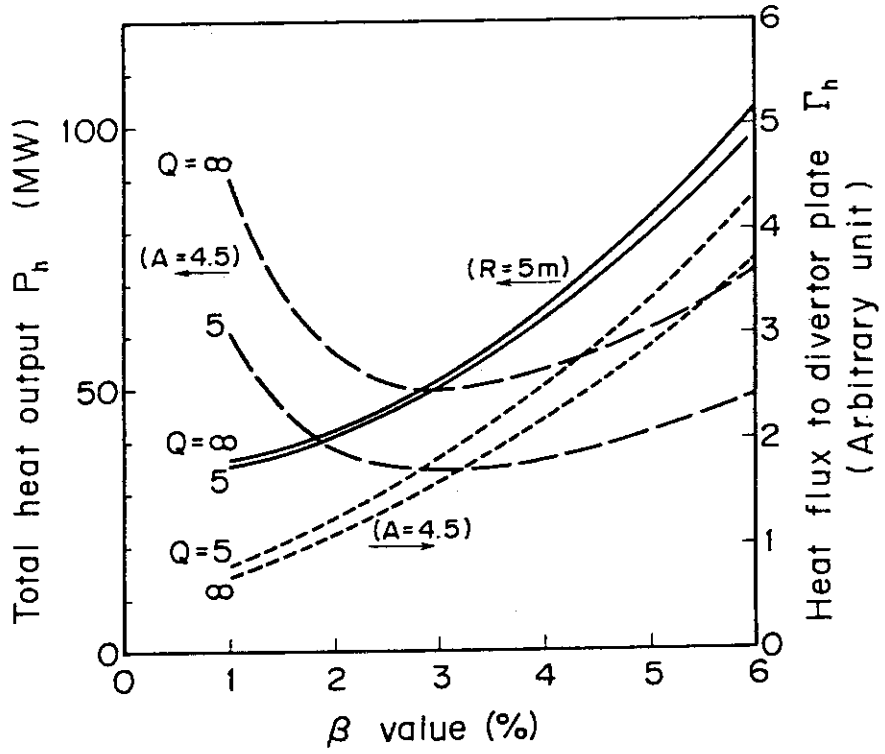


Fig. 4.6 Total heat output  $P_h$  ( $\alpha$  heating and external heating) and heat flux to divertor plate  $\Gamma_h$  as a function of  $\beta$  value for various plasma performance ( $Q=5$  and  $\infty$ ). Major radius  $R$  or aspect ratio  $A$  is fixed ( $R=5m$  or  $A=4.5$ ).

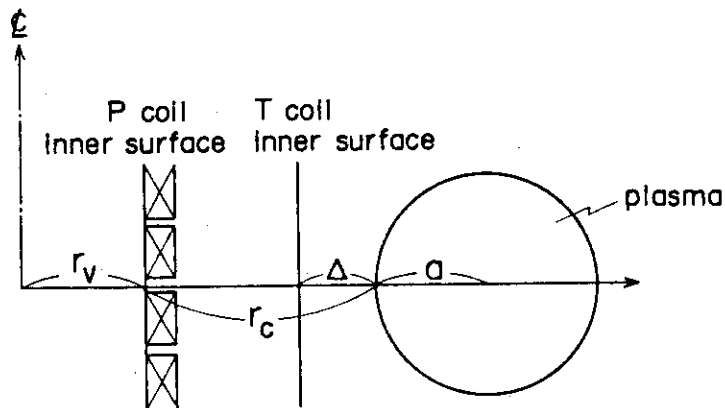


Fig. 4.7 Schematic drawing of the required space of the device.  $r_v$ : volt seconds.  $r_c$ : P and T coils, support structure, shield, vacuum vessel.  $\Delta$ : shield and vacuum vessel.

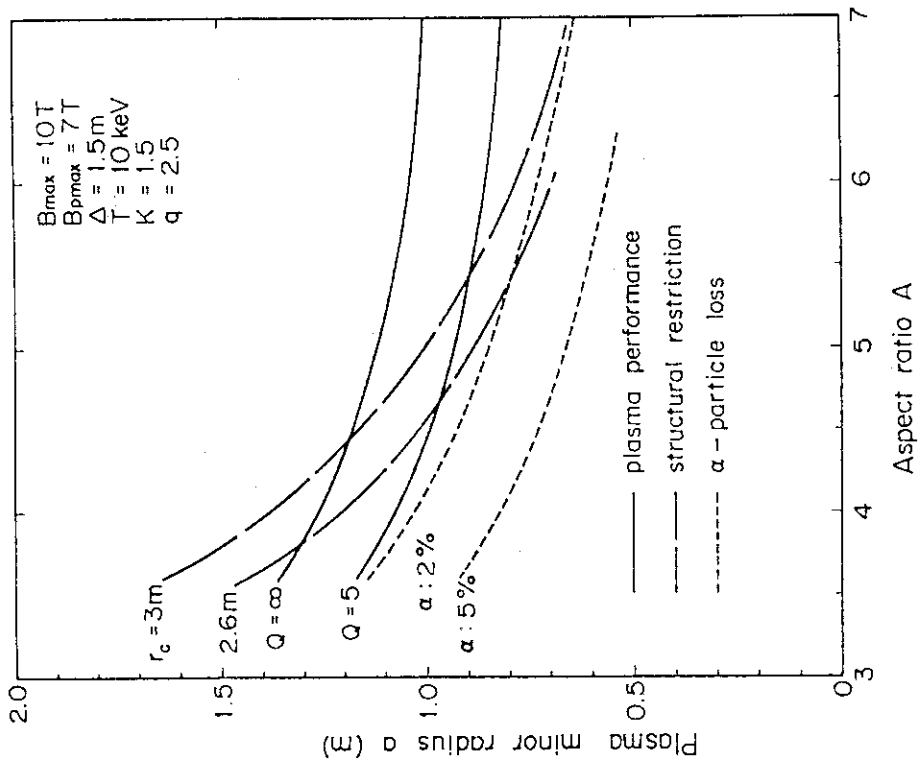


Fig. 4.9 Device sizes to realize the required plasma performances ( $Q=5$  and  $\infty$ ), to meet the structural restriction on aspect ratio for  $B_{max}=10T$ ,  $B_{pmax}=7T$  and  $\Delta=1.5m$ . Device sizes for constant  $\alpha$ -particle orbit loss ( $G_{loss}=2\%$  and  $5\%$ ) are also shown.

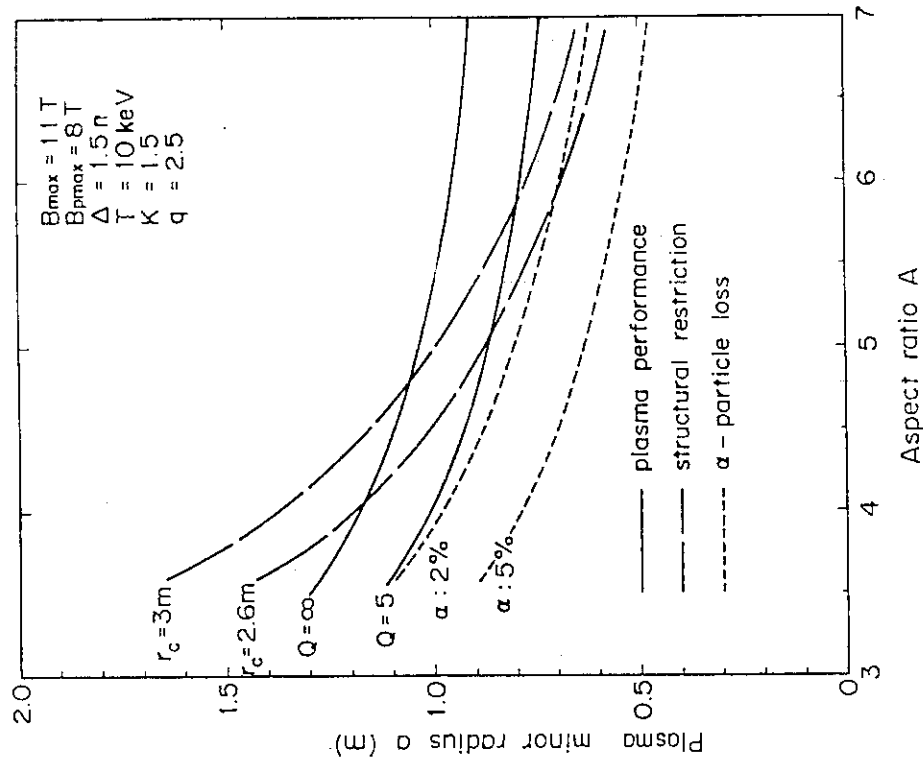


Fig. 4.8 Device sizes to realize the required plasma performances ( $Q=5$  and  $\infty$ ), to meet the structural restriction on aspect ratio for  $B_{max}=11T$ ,  $B_{pmax}=8T$  and  $\Delta=1.5m$ . Device sizes for constant  $\alpha$ -particle orbit loss ( $G_{loss}=2\%$  and  $5\%$ ) are also shown.



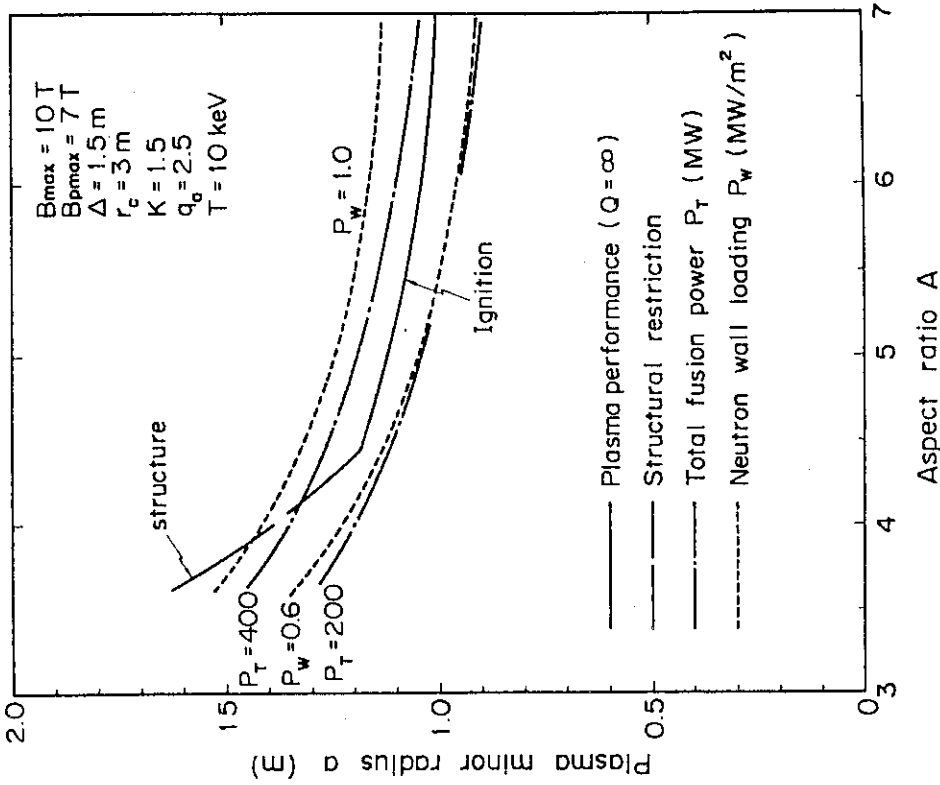


Fig. 4.11 The region of the device sizes to realize the self-ignition condition, the required total fusion power ( $P_T=200$  and  $400\text{MW}$ ), the required neutron wall loading ( $P_W=0.6$  and  $1\text{MW}/\text{m}^2$ ) and to meet the structural restriction on aspect ratio for  $B_{\text{max}}=10\text{T}$ ,  $B_{\text{pmax}}=7\text{T}$  and  $\Delta=1.5\text{m}$ .

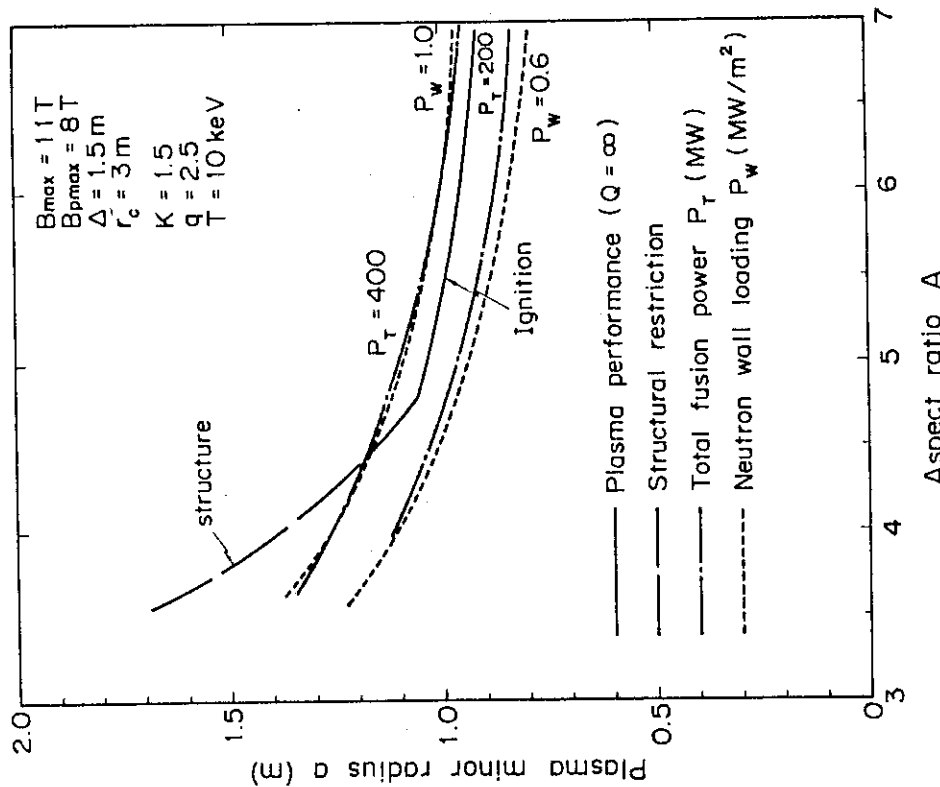


Fig. 4.10 The region of the device sizes to realize the self-ignition condition, the required total fusion power ( $P_T=200$  and  $400\text{MW}$ ), the required neutron wall loading ( $P_W=0.6$  and  $1\text{MW}/\text{m}^2$ ) and to meet the structural restriction on aspect ratio for  $B_{\text{max}}=11\text{T}$ ,  $B_{\text{pmax}}=8\text{T}$  and  $\Delta=1.5\text{m}$ .

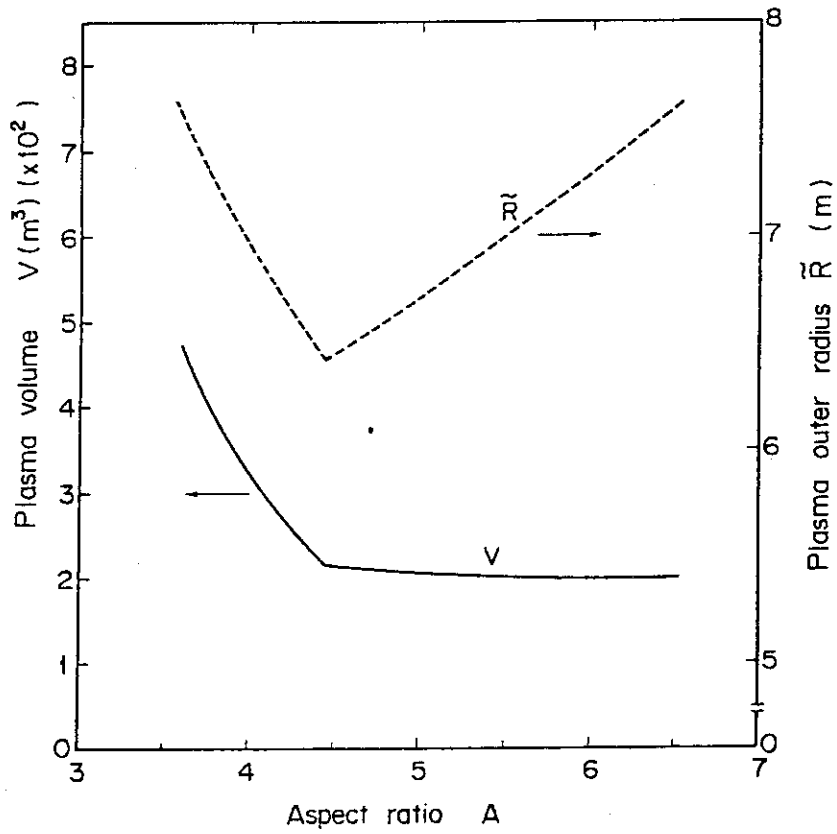


Fig. 4.12 Plasma volume  $V$  and plasma outer radius  $\bar{R}$  as a function of aspect ratio on the contour of the structural restriction and self-ignition condition in Fig. 4.11.

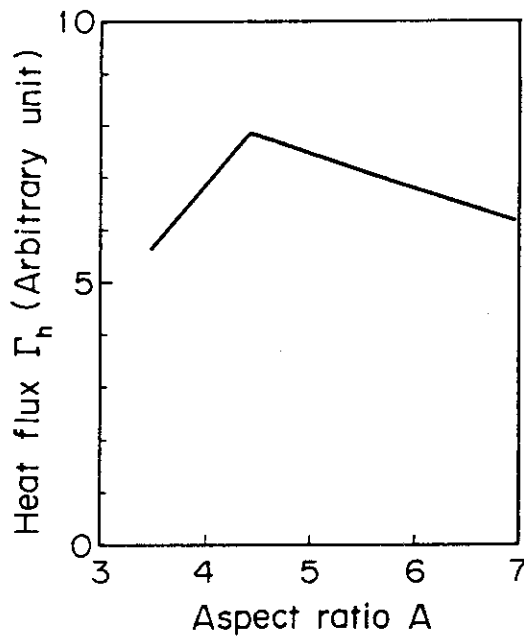


Fig. 4.13 Heat flux to divertor plate as a function of aspect ratio on the same contour as in Fig. 4.12.

## Acknowledgement

The authors would like to thank Drs. M. Tanaka, K. Itoh, K. Sako, Y. Shimomura, T. Tuda and H. Maeda for their valuable discussions and comments. They are also grateful to Drs. K. Shinya, K. Ueda, S. Saito and A. Hatayama for their collaborations of the work. It is our pleasure to thank Drs. T. Hiraoka, M. Yoshikawa, K. Tomabechi, Y. Iso and S. Mori for their valuable comments and continuous encouragements throughout the work.

## References

- (1) INTOR Group, in INTOR zero phase report, IAEA, VIENNA (1980).  
Nuclear Fusion 29 (1980) 349.
- (2) M. Azumi, et al., "Evolution of Stable High Beta Tokamak Equilibria",  
8th Int. Conf. on Plasma Physics and Controlled Nuclear Fusion Research,  
Brussels, 1980, IAEA-CN-38/K-1-1.
- (3) Suzuki N., et al., 8th Int. Conf. on Plasma Physics and Controlled Nuclear  
Fusion Research, Brussels, 1980, IAEA-CN-38/T-2-3.
- (4) M. Tanaka, et al.: to be published.
- (5) K. Sako, et al.: JAERI-M 8518 (1979).
- (6) T. Hiraoka, et al.: JAERI-M 8198 (1979).
- (7) K. Sako, et al.: JAERI-M 7300 (1977), JAERI-M 8286 (1979).
- (8) T. Takizuka, et al.: JAERI-M 9354 (1981).
- (9) T. Tuda, et al.: private communications.
- (10) T. Takizuka, et al.: JAERI-M 8621 (1980).
- (11) T. Tuda : private communications.

## Acknowledgement

The authors would like to thank Drs. M. Tanaka, K. Itoh, K. Sako, Y. Shimomura, T. Tuda and H. Maeda for their valuable discussions and comments. They are also grateful to Drs. K. Shinya, K. Ueda, S. Saito and A. Hatayama for their collaborations of the work. It is our pleasure to thank Drs. T. Hiraoka, M. Yoshikawa, K. Tomabechi, Y. Iso and S. Mori for their valuable comments and continuous encouragements throughout the work.

## References

- (1) INTOR Group, in INTOR zero phase report, IAEA, VIENNA (1980).  
Nuclear Fusion 29 (1980) 349.
- (2) M. Azumi, et al., "Evolution of Stable High Beta Tokamak Equilibria",  
8th Int. Conf. on Plasma Physics and Controlled Nuclear Fusion Research,  
Brussels, 1980, IAEA-CN-38/K-1-1.
- (3) Suzuki N., et al., 8th Int. Conf. on Plasma Physics and Controlled Nuclear  
Fusion Research, Brussels, 1980, IAEA-CN-38/T-2-3.
- (4) M. Tanaka, et al.: to be published.
- (5) K. Sako, et al.: JAERI-M 8518 (1979).
- (6) T. Hiraoka, et al.: JAERI-M 8198 (1979).
- (7) K. Sako, et al.: JAERI-M 7300 (1977), JAERI-M 8286 (1979).
- (8) T. Takizuka, et al.: JAERI-M 9354 (1981).
- (9) T. Tuda, et al.: private communications.
- (10) T. Takizuka, et al.: JAERI-M 8621 (1980).
- (11) T. Tuda : private communications.